

Explanation Space: A New Perspective into Time Series Interpretability

Shahbaz Rezaei, Xin Liu

¹University of California
Davis, CA, USA
srezaei@ucdavis.edu, xinliu@ucdavis.edu

Abstract

Human understandable explanation of deep learning models is necessary for many critical and sensitive applications. Unlike image or tabular data where the importance of each input feature (for the classifier’s decision) can be directly projected into the input, time series distinguishable features (e.g. dominant frequency) are often hard to manifest in time domain for a user to easily understand. Moreover, most explanation methods require a baseline value as an indication of the absence of any feature. However, the notion of lack of feature, which is often defined as black pixels for vision tasks or zero/mean values for tabular data, is not well-defined in time series. Despite the adoption of explainable AI methods (XAI) from tabular and vision domain into time series domain, these differences limit the application of these XAI methods in practice. In this paper, we propose a simple yet effective method that allows a model originally trained on time domain to be interpreted in other *explanation spaces* using existing methods. We suggest four explanation spaces that each can potentially alleviate these issues in certain types of time series. Our method can be readily adopted in existing platforms without any change to trained models or XAI methods. The code is available at <https://github.com/shrezaei/TS-X-spaces>.

Introduction

Explainable AI (XAI) is a recent branch of studies dedicated to provide human interpretable explanation of deep models. Initially introduced for image data, attribution-based methods aim to highlight the region of the image responsible for the model’s decision. Similar approach has been later adopted for other data types, including time series. However, unlike a typical image, time series are vastly diverse in nature. In many cases, the associated feature cannot be easily presented in time domain (Schröder, Zamanian, and Ahmidi 2023), such as dominant frequency, Hurst parameter, Lyapunov exponent, etc. In such cases, a classifier can achieve high accuracy while XAI methods are inevitably doomed to provide understandable explanation. For instance, the representation in time versus frequency domain of a model trained on FordA dataset is shown in Figure 1a and 1b which clearly shows that only a few frequency components are

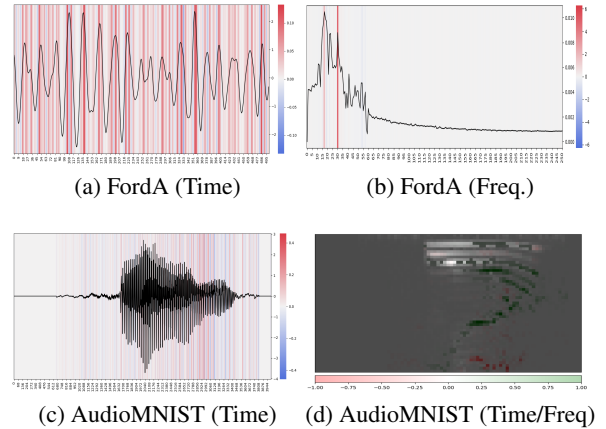


Figure 1: DeepLIFT attribution method on FordA and AudioMNIST datasets.

dominant, and thus more desirable, while the time domain explanation is more complex and hard to comprehend. Similarly, an audio signal the time/frequency space (Figure 1d) generates a more sparse explanation than the time domain (Figure 1c).

In this paper, our premise is that a more **sparse** explanation is more interpretable to an end user. Our key observation is that different spaces generate explanation with different sparsity on different type of time series that is aligned with our intuitive understanding of the nature of time series. The main challenge is that how to explain an existing DL model trained only on time domain in different domains.

To address this challenge, we introduce the concept of explanation space projection, where a simple procedure allows existing XAI methods to explain a model in different spaces¹, such as time, frequency, or time/frequency. Using this procedure, we can generate explanations in multiple domains and automatically select the most appropriate space with respect to a chosen metric, such as sparsity. The main advantage of our method is that the target DL model is not required to be retrained on any other space. In other words, an existing model trained on any domain can be explained

¹In this paper, we use domain and space, interchangeably.

in all other domains using any existing XAI method. As a result, it can be easily adopted and used in practice.

We show that the explanation spaces are not limited to the well-known time and frequency spaces. In fact, any one-to-one function can introduce a new explanation space. To show the usefulness of this generalization in practice, we introduce two new explanation spaces, namely, min-zero and difference spaces, each suitable for certain types of time-series, and addressing the baseline problem. We evaluate our method on nine XAI methods using three DL models and different types of time series, including sensor data, audio, and motion, and illustrate the usefulness of different spaces in explaining different types of time series with less complexity.

Related Work

This paper focuses on post-hoc explanation methods. There are several mechanisms to generate an explanation: Using gradient, such as Integrated Gradient (Sundararajan, Taly, and Yan 2017), GradientSHAP (Erion et al. 2020), DeepLIFT (Shrikumar, Greenside, and Kundaje 2017), DeepSHAP (Lundberg and Lee 2017), Saliency (Simonyan, Vedaldi, and Zisserman 2013), InputXGradient (Shrikumar et al. 2016), Guided BackProp (Springenberg et al. 2014), and KernelSHAP (Lundberg and Lee 2017), or occluding features, such as Feature Occlusion (Zeiler and Fergus 2014), and feature ablation (Suresh et al. 2017). Most early works were originally developed for computer vision. Recently, some explanation methods are proposed to deal with challenges in time series data, such as TSR (Ismail et al. 2020), Demux (Doddaiyah et al. 2022), TimeX (Queen et al. 2024), LEFTIST (Guilleme et al. 2019), MILLET (Early et al. 2023), or DFT-LPR (Vielhaben et al. 2024). All these methods, and majority of computer vision methods, are attribution-based highlighting the importance of each pixel/time-step to the prediction.

In this paper, we focus on a new concept, i.e. explanation space, rather than a new explanation method. The closest work in literature is DFT-LPR (Vielhaben et al. 2024) where the authors proposed a virtual inspection layer at the beginning of a model trained on time domain. They adopted LPR (Bach et al. 2015) method such that it propagates the relevance back to the frequency or time/frequency domain. However, this method only works with LPR and also doesn't easily allow new spaces to be introduced. In this paper, we solve this limitation by introducing a generalized wrapping mechanism that changes the input type of a model without changing its functionality. Hence, any existing XAI method can be used to generate explanation in the new input type.

Method

Let $x = \{x_1, x_2, \dots, x_N\} \in R^N$ be a time series sample, where x_i is the value at time step i and N is the number of time steps. To each time series sample there is a label associated, denoted by $y \in \{y_1, \dots, y_C\}$ where C is the number of classes. A classifier, $M : x \rightarrow y$, maps a times series sample to a probability distribution vector over C classes. An explanation method, $E(M(\cdot), x) \rightarrow \bar{x}$, takes a classifier

and a time series sample and generates an output, \bar{x} . In the case of attribution methods, \bar{x} is a heat-map with the same dimension as x , and in the case of counterfactual methods, \bar{x} is a new time series where $M(x) \neq M(\bar{x})$.

Reversible Representation Space: A one-to-one function F , with a reverse function F^{-1} , is a representation space and it implies that $F^{-1}(F(x)) = x$. In this paper, we also refer to it as an **explanation space** since we mainly focus on changing a domain for the purpose of explanation.

Projection of Explanation from Time Domain into a New Explanation Space: Assume a classifier M trained on time domain. Consider an explanation space F (e.g. FFT where it outputs frequency domain). Since $M(F^{-1}(F(x))) = M(x)$, we can define $z = F(x)$ as a new domain and the associated classifier is $M'(z) = M(F^{-1}(z)) \rightarrow y$. The new classifier M' is the same as M except that it performs the reverse operation, F^{-1} , before passing the input to M . Hence, M on x domain is functionally the same as M' on z . However, now, we can use any existing explanation method, E , to generate an explanation on z domain (or on explanation space F) using $E(M'(\cdot), z)^2$.

Explanation Spaces

The projection procedure allows us to generate an explanation on any explanation space even if the original model is only trained on time domain. Here, we introduce a few explanation spaces useful in certain applications:

Frequency Space is the Fourier transform and the reverse function is the inverse Fourier transform. As explained in Introduction, FordA dataset is an example where the frequency domain explanation is less complex than time (Figure 1b versus 1a).

Time/Frequency Space is the short-time discrete Fourier transform to allow the explanation on both time and frequency domains. Figure 1c shows the attribution generated by DeepLIFT on AudioMNIST (Becker et al. 2023) in time domain and Figure 1d shows the attribution generated by the same method on time/frequency domain. The attribution on time/frequency domain is more focused on the center of the time series where actual signal is presented.

Min Zero Space aims to alleviate the well-known issue of baseline exist on many attribution-based methods (Höllig, Thoma, and Grimm 2023). By default, many existing explanation methods implicitly or explicitly assume a specific value (zero for the most part or a value set by user or training set) to be associated with a lack of any feature, including InputXGradient, feature occlusion, DeepLIFT, etc. Because time series are often z-normalized per sample to have a zero mean mainly for training stability, the zero value does not correspond to the lack of feature even if the original un-normalized time series does. For example, power consumption time series (e.g. ElectricDevices and LargeKitchenAppliances datasets in UCR repository) or time series dataset containing number of events or magnitude of events (e.g. Earthquakes and ChinaTown datasets in UCR repository or

²It is desirable for F/F^{-1} to be almost everywhere differentiable. Otherwise, gradient-based explanation methods may fail.

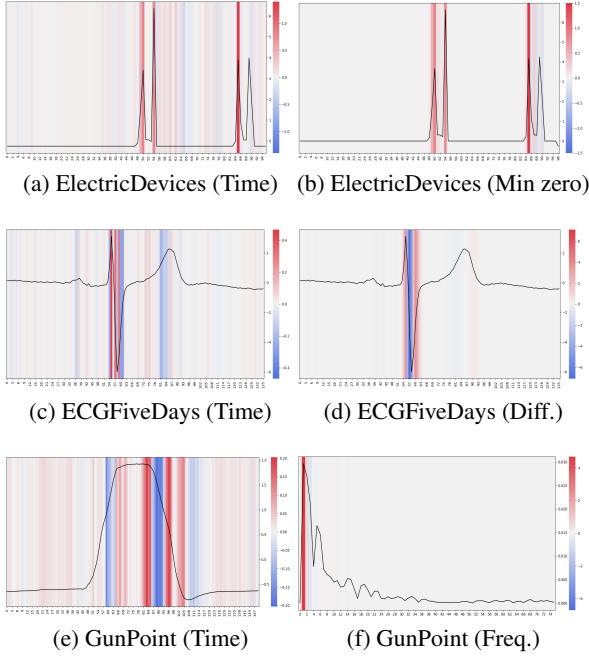


Figure 2: DeepLIFT attribution method on ElectricDevices, ECGFiveDays, and GunPoint datasets.

network traffic classification (Rezaei and Liu 2020)) are examples of natural time series where zero corresponds to a lack of feature/event in the unnormalized version, but not in the normalized one. This causes many artifacts to appear in XAI methods as shown in Figure 2a. This is consistent with the observation in (Samek et al. 2019) that a global mean shift in data changes the explanation.

Min zero space maps the normalized time series on time domain to a min zero space where the minimum value is set back to zero such that it represents the lack of feature. To do so, F_{min_zero} shifts the entire time series such that the min is zero and then stores the previous min value in an extra time step at the end so that the reversible operation is possible, as follows:

$$F_{min_zero}(\{x_1, x_2, \dots, x_N\}) \rightarrow \{x_1 - x_{min}, x_2 - x_{min}, \dots, x_N - x_{min}, x_{min}\} \quad (1)$$

where x_{min} is the minimum value in the normalized time series. Note that the reverse operation (F^{-1}) is needed to be embedded into a new neural network, $M(F^{-1}(\cdot))$. This can be easily done by adding a single fully connected layer before $M(\cdot)$ where it adds the last element to the first N elements. The implementation of the weight matrix associated with such a fully connected layer is explained in Appendix. As shown in Figure 2b, generating the attribution on mean zero space using the same method as Figure 2a completely removes all artifacts assigned to the part with no signal.

Note that, for some XAI methods, one can set minimum as a baseline value and generate an explanation in time domain similar to an explanation in min zero space, such as DeepLIFT or Occlusion. However, this is not true for all

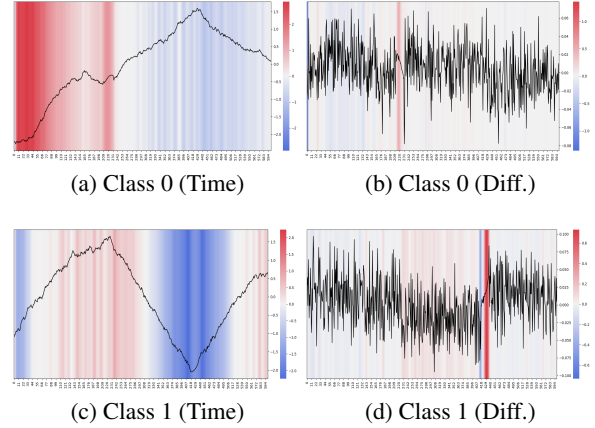


Figure 3: Occlusion XAI on a non-stationary dataset.

XAI methods, including Saliency which doesn't take a baseline, InputXGradient where the baseline is always implied to be zero, Integrated Gradient where the integral is taken over a range which may or may not include (start from) a target baseline, etc. In other words, the mean zero space provides a more general mechanism that allows all XAI methods to address the baseline issue for this type of TS.

Difference Space is a result of taking a difference of each two consecutive time steps as a new time series. Differencing has been widely used in time series analysis to remove a trend or to make a time series stationary (Hyndman and Athanasopoulos 2018). In our framework, difference domain has two benefits. First, for non-stationary time series (often with trend), such as stock price or atmospheric time series, a shapelet-like feature in a small region can be completely imperceptible. For example, in a synthetic data generated to mimic a non-stationary time series with a small shapelet as a distinguishable feature, a shapelet feature may not be easily visible when it is small in comparison to the range of the entire time series³, as shown in Figure 3a and 3c. However, the shapelets (i.e. semi-linear increase/decrease patterns visible in difference domain where the long range fluctuations is effectively removed, as shown in the corresponding samples in Figure 3b and 3d. Interestingly, the difference and time domain has a huge impact on the performance of XAI methods. The XAI method completely fails the time domain which can be explained by the second benefit.

Second, the difference domain implicitly changes the notion of a feature. Here, the lack of change in time domain corresponds to zeros in difference domain (implying a lack of feature), and changes correspond to non-zeros values. This can solve the baseline issue for certain types of time series. For example, in time series associated with movements (e.g. GunPoint) or ECG signals, the lack of activity is better manifested by a sequence of near constant values, not

³We use synthetic data in this experiment since there is no dataset with such properties in UCR repository or any publicly available classification repository we are aware of.

necessarily a sequences of zeros. By taking the difference of the time series, a sequence of unchanging values will map to a sequence of zeros and, hence, aligns with the most explanation methods’ baselines. Formally, the difference space is defined as

$$F_{diff}(\{x_1, x_2, \dots, x_N\}) \rightarrow \{x_1, x_2 - x_1, x_3 - x_2, \dots, x_N - x_{N-1}\} \quad (2)$$

The reverse operation is trivial and the fully connected implementation is explained in Appendix. Figure 2c and 2d shows the attribution generated by DeepLIFT on time domain and difference domain, respectively. Note that in Figure 2d we show the attribution generated on difference space on top of the time domain just for better visualization. In reality, the difference domain time series looks different from the original time domain. As shown, the difference space’s explanation is sparser and focuses on the actual heartbeat of the ECG signal.

Evaluation

Experimental Setup: We include several datasets covering different types of time series, as shown in Table 1, mainly from UCR Repository (Dau et al. 2019) except AudioMNIST provided in (Vielhaben et al. 2024). For each dataset, we trained two commonly used model architectures: a ResNet⁴ and an InceptionTime model (Ismail Fawaz et al. 2020). We emphasize that all models are trained only on time domain. The explanations are generated on different domain using the process described in Method Section. We evaluate nine well-known XAI methods: DeepLIFT, GradientSHAP, Guided BackProp (Springenberg et al. 2014), InputXGradient (I×G), Integrated Gradient (IG), KernelSHAP, LIME (Ribeiro, Singh, and Guestrin 2016), Occlusion, and Saliency (Simonyan, Vedaldi, and Zisserman 2013). We use Captum implementation (Kokhlikyan et al. 2020) for XAI methods.

Note that the goal of this paper is not to have comprehensive evaluation of different XAI methods, as it has previously shown that no single XAI method can outperform others in all metrics/datasets (Löffler et al. 2022). Rather, we focus on illustrating that the concept of spaces is useful and that the same XAI method may bring a better explanation (with respect to some metric such as sparsity) on different spaces depending on the type of time series. While our method can be easily adopted for existing counter-factual XAI methods as well, such evaluation is the subject of future studies.

Evaluation Criteria

Robustness: Robustness of an attribution method refers to its sensitivity with respect to small perturbations of the target sample (Höllig, Thoma, and Grimm 2023; Löffler et al. 2022). Unlike previous studies, we investigate the effect of different input spaces. As a result, a trained model wrapped to take frequency domain input may be more sensitive than

⁴ResNet implementation for time series is adopted from TSEvo package (Höllig, Kulbach, and Thoma 2022).

Dataset	Type	ResNet	InceptionTime
AudioMNIST	Audio	87.47%	90.68%
FordA	Sensor	93.56%	93.41%
GunPoint	Motion	100%	99.33%
ECGFiveDays	ECG	91.29%	100%
ECG5000	ECG	93.24%	94.47%
LargeKitchenAppliance	Device	85.87%	88.00%
ElectricDevices	Device	73.17%	71.22%
Earthquakes	Sensor/Event	73.38%	74.82%

Table 1: Dataset types and models’ accuracy

the unwrapped version taking the time domain input. It is not trivial whether a model wrapped in other domains is more sensitive to perturbation than time domain or not. Hence, we also need to evaluate the sensitivity of the model itself in different input spaces. So, unlike previous work, we define two robustness: the first one is associated with the classifier and the second one is associated with the XAI method. *Classifier robustness* is defined as follow:

$$Rbt_{cls} = |M_c(x) - M_c(x + \lambda\epsilon)| \quad (3)$$

where subscript c indicates the probability output of the model for class c , the predicted class for sample x . Similar to (Höllig, Thoma, and Grimm 2023), the XAI method’s robustness is defined as follows:

$$Rbt_{xai} = \frac{1}{|x|} ||E(M(\cdot), x) - E(M(\cdot), x + \lambda\epsilon)|| \quad (4)$$

In our experiments, we take the average over 10 random perturbations. The perturbation, ϵ , follows Gaussian distribution with zero mean and standard deviation equal to the input space’s standard deviation, and λ is set to 0.01.

Faithfulness: An explanation is faithful if the input features with highest attributions have the most effect on the prediction (Löffler et al. 2022). We measure the faithfulness using percentage of samples for which the prediction label flips when all non-negligible attributions are replaced with a default value, as follows:

$$Faith = 1 - \mathbb{1}_{M(x)}\{M(P(x, E, \epsilon))\} \quad (5)$$

where E is the attribution generated using sample x and the model M , $\mathbb{1}_{M(x)}$ is the indicator function that return 1 when prediction class of $M(x)$ and $M(P(x, E, n))$ matches and zero otherwise, and $P(x, E, n)$ is the masking function that zero out input features of x with attribution greater than ϵ . Although the metric returns a boolean for a single sample, when taking the average over entire dataset, it shows the percentage of successful flip as a measure of faithfulness.

In literature, some studies proposed using values rather than zero as a default baseline, either for generating explanation or measuring faithfulness. For example, (Löffler et al. 2022) replaces a time step with the average value of that time step in training set (which is not a practical assumption for shift-variant time series), (Schlegel et al. 2019) picks a subsequence and reverses the time orders of the time steps, and (Parvatharaju et al. 2021) learns the most useful replacement/perturbation from the training data, etc. Such assumptions

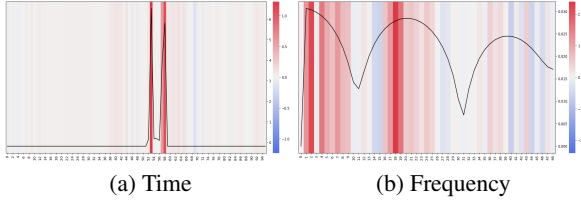


Figure 4: DeepLIFT on ElectricDevices dataset. While the Shannon entropy indicates less complexity for the frequency domain (3.35 versus 3.50), our sparsity metric indicates less complexity for time domain (0.80 versus 0.40).

are always data type dependent. We avoid the baseline problem in all non-time domain spaces by defining them in such a way that zero has a specific meaning corresponding to certain lack of features. However, whether a certain space is suitable for a target dataset needs to be carefully considered by a practitioner familiar with that type of time series.

Sparsity: In time series explanation, sparsity (also known as complexity) is often defined using Shannon entropy (Höllig, Thoma, and Grimm 2023; Vielhaben et al. 2024). Despite its wide usage, it has a few limitations. First, it does not have a predefined upper limit. In other words, for a given dataset, Shannon entropy is always between zero and a positive real number that depends on the length of the time series. Because the upper limit is not fixed and predefined, it is hard for an XAI user to internalize how complex an explanation is in an absolute sense. Another problem with Shannon entropy is its *length-dependent accumulation of extremely small non-zero attributions*. A motivating example of why the length matters is shown in Figure 4. Since the length of the input in time domain is twice the length in frequency domain and because the attribution in time domain contains many small non-zero values, all non-zero values accumulate resulting in the higher Shannon entropy in time domain. This is in stark contrast to what is visually presented. Our formulation (in equation (6)), however, indicates better sparsity in time domain since it takes the length into account.

Last, ignoring the length may have other consequences. For example, imagine two different input domains, X_1 and X_2 , where the length of the first one is larger than the second one, i.e. $l_1 \gg l_2$. If an XAI method assigns high attribution to two input features and zero to others in both input domains, Shannon entropy of the two explanations is equal. However, picking out two input features in a space where the length of the input is larger is more significant. Although this was not a problem in previous studies due to the fix length of the time domain, in our evaluation we need a metric sensitive to the input length because some explanation spaces, such as frequency and time/frequency, have different lengths than the corresponding time domain. We note that the choice of an explanation space and what metric is appropriate is not trivial and depends on the nature of the application. Hence, a practitioner should choose a suitable option accordingly.

Here, we introduce four desirable properties for a sparsity

metric and then propose a new simple metric that satisfies all properties. A sparsity metric, $Spr(\cdot)$, should satisfy:

1. Sparsity is bounded, i.e. $0 \leq Spr(E(x)) \leq 1$, where greater values mean more sparsity (i.e. less complexity).
2. A complete uniform attribution has zero sparsity, i.e. if $E_i(x) = E_j(x)$ for all $1 \leq i, j \leq n$, then $Spr(E(x)) = 0$. Here, E_i indicates the attribution at input feature i .
3. An explanation with single non-zero attribution at i and zero elsewhere has a sparsity value of 1, i.e. if $E_i(x) \neq 0$ and $E_j(x) = 0$ (where $j \neq i$), then $Spr(E(x)) = 1$.
4. If two explanations have the same sparsity measure for the non-zero part of the attribution but one has more zero attributions, the longer one is more sparse. In other words, if $Spr(E^{\neq 0}(x)) = Spr(E^{\neq 0}(x'))$ and $|E^{\neq 0}(x)| > |E^{\neq 0}(x')|$, where $E^{\neq 0}$ and $E^{\neq 0}$ means the non-zero and zero portion of the attribution, respectively, then $Spr(E(x)) > Spr(E(x'))$.

Assuming that an attribution, $E(x)$ is min-max normalized such that $0 \leq E_i(x) \leq 1^5$, we define the sparsity metric as follows:

$$Spr(E(x)) = \left(\frac{\sum_{i=1}^n (1 - E_i(x))}{n - 1} \right)^\beta \quad (6)$$

where $\beta > 1$ is a constant hyper-parameter to spread out the metric more uniformly. It is easy to show that it satisfies all above properties. See Appendix for more details.

Sparsity on Different Spaces

In Table 2, we report sparsity along the faithfulness success percentage to roll out sparse but non-faithful explanations. Here, the first number is the success percentage and the number in the parenthesis is the sparsity. We exclude the sparsity for entries with lower than 50% success percentage. For most datasets, LIME only picks a few input features (regardless of the input space) and produces a highly sparse explanation. However, most explanations turn out to be irrelevant in terms of faithfulness. Note that we use default hyper-parameters when possible for all XAI methods. It is possible to make some methods better by tuning the parameters. For example, by grouping each m consecutive time steps as a single feature, LIME can generate more faithful explanation. However, such a hyper-parameter search is not only beyond the scope of this paper, but also unnecessary for the purpose of this paper. We emphasize that our goal is to show that the same XAI method can be used on different explanation spaces and generate different quality explanation.

As shown in Table 2, different XAI methods may produce the most sparse explanation in different spaces. So, the sparsity is not always consistent. Nevertheless, the sparsity pattern aligns with our intuition when we proposed explanation spaces. For example, AudioMNIST, containing audio signals, is the most sparse in time/frequency domain in 6 out of 8 faithful methods and the two others are frequency spaces. FordA, a dataset of engine noises, is most sparse in

⁵If attribution is the same over all time steps, the min-max normalization outputs a sequence of ones.

Dataset	Domain	DeepLIFT	GradientSHAP	G. Backprop	$I \times G$	IG	Kernel SHAP	LIME	Occlusion	Saliency
AudioMNIST	Time	88% (0.87)	88% (0.83)	75% (0.75)	88% (0.88)	88% (0.87)	87% (0.78)	0% (-)	94% (0.67)	81% (0.81)
	Freq.	97% (0.87)	94% (0.89)	99% (0.91)	95% (0.86)	96% (0.86)	75% (0.94)	34% (-)	97% (0.62)	99% (0.80)
	Time/Freq.	100% (0.93)	99% (0.91)	99% (0.84)	100% (0.93)	75% (0.93)	91% (0.82)	15% (-)	100% (0.94)	92% (0.84)
	Difference	90% (0.88)	90% (0.81)	100% (0.07)	90% (0.88)	90% (0.88)	90% (0.87)	45% (-)	93% (0.75)	100% (0.21)
	Min Zero	90% (0.75)	90% (0.71)	98% (0.75)	89% (0.82)	91% (0.76)	98% (0.66)	2% (-)	81% (0.94)	88% (0.81)
FordA	Time	52% (0.58)	51% (0.53)	52% (0.39)	51% (0.59)	51% (0.58)	51% (0.39)	6% (-)	57% (0.24)	51% (0.46)
	Freq.	97% (0.92)	61% (0.89)	94% (0.92)	90% (0.92)	98% (0.90)	63% (0.67)	14% (-)	85% (0.88)	82% (0.89)
	Time/Freq.	100% (0.87)	84% (0.84)	75% (0.78)	100% (0.87)	90% (0.83)	82% (0.58)	20% (-)	96% (0.91)	97% (0.66)
	Difference	51% (0.43)	51% (0.42)	51% (0.10)	51% (0.45)	51% (0.43)	51% (0.73)	49% (-)	52% (0.34)	51% (0.11)
	Min Zero	51% (0.44)	51% (0.54)	51% (0.39)	51% (0.46)	51% (0.40)	51% (0.40)	26% (-)	52% (0.87)	51% (0.46)
GunPoint	Time	50% (0.44)	50% (0.52)	52% (0.24)	50% (0.44)	50% (0.48)	58% (0.46)	12% (-)	74% (0.20)	60% (0.44)
	Freq.	68% (0.92)	54% (0.83)	86% (0.92)	54% (0.88)	64% (0.88)	64% (0.49)	38% (-)	82% (0.79)	96% (0.81)
	Difference	64% (0.65)	62% (0.55)	66% (0.11)	66% (0.64)	70% (0.69)	58% (0.44)	4% (-)	86% (0.51)	76% (0.13)
	Min Zero	48% (-)	64% (0.56)	52% (0.24)	66% (0.60)	54% (0.60)	68% (0.44)	22% (-)	66% (0.20)	70% (0.44)
ECGFiveDays	Time	39% (-)	43% (-)	43% (-)	39% (-)	39% (-)	39% (-)	26% (-)	61% (0.43)	39% (-)
	Freq.	61% (0.67)	74% (0.58)	100% (0.77)	70% (0.68)	83% (0.63)	78% (0.55)	17% (-)	87% (0.40)	100% (0.61)
	Difference	78% (0.81)	65% (0.80)	26% (-)	74% (0.80)	96% (0.82)	83% (0.48)	35% (-)	100% (0.61)	87% (0.19)
	Min Zero	96% (0.40)	83% (0.55)	100% (0.40)	83% (0.44)	96% (0.42)	52% (0.40)	39% (-)	61% (0.07)	100% (0.43)
ECG5000	Time	4% (-)	4% (-)	3% (-)	5% (-)	5% (-)	3% (-)	1% (-)	95% (0.28)	85% (0.44)
	Freq.	44% (-)	25% (-)	82% (0.81)	19% (-)	54% (0.76)	35% (-)	8% (-)	75% (0.50)	89% (0.65)
	Difference	100% (0.83)	99% (0.76)	70% (0.11)	100% (0.82)	100% (0.80)	98% (0.50)	74% (0.81)	100% (0.75)	99% (0.17)
	Min Zero	100% (0.37)	98% (0.45)	100% (0.40)	100% (0.46)	100% (0.37)	99% (0.33)	75% (0.81)	100% (0.45)	97% (0.44)
LargeKit.App.	Time	61% (0.94)	67% (0.90)	62% (0.87)	64% (0.93)	52% (0.94)	58% (0.40)	3% (-)	82% (0.49)	94% (0.68)
	Freq.	88% (0.78)	61% (0.77)	84% (0.75)	79% (0.84)	60% (0.80)	57% (0.72)	38% (-)	97% (0.65)	87% (0.80)
	Time/Freq.	99% (0.96)	68% (0.90)	38% (-)	94% (0.94)	100% (0.95)	49% (-)	30% (-)	67% (0.90)	82% (0.79)
	Difference	84% (0.96)	85% (0.92)	82% (0.16)	84% (0.96)	84% (0.96)	92% (0.51)	49% (-)	99% (0.94)	100% (0.07)
	Min Zero	65% (0.96)	52% (0.92)	61% (0.87)	64% (0.96)	51% (0.96)	72% (0.69)	3% (-)	69% (0.89)	80% (0.68)
ElectricDev.	Time	100% (0.67)	100% (0.62)	79% (0.50)	99% (0.68)	100% (0.67)	100% (0.32)	70% (0.76)	100% (0.24)	100% (0.44)
	Freq.	98% (0.60)	92% (0.51)	100% (0.44)	95% (0.54)	98% (0.54)	88% (0.42)	80% (0.74)	99% (0.27)	99% (0.48)
	Difference	99% (0.65)	100% (0.64)	85% (0.11)	99% (0.64)	99% (0.64)	99% (0.45)	79% (0.72)	99% (0.47)	99% (0.14)
	Min Zero	67% (0.77)	75% (0.67)	79% (0.50)	71% (0.78)	75% (0.77)	65% (0.43)	40% (0.76)	92% (0.60)	85% (0.45)
Earthquakes	Time	82% (0.87)	73% (0.79)	79% (0.81)	78% (0.84)	82% (0.85)	50% (0.71)	2% (-)	77% (0.65)	68% (0.70)
	Freq.	100% (0.62)	97% (0.61)	99% (0.56)	100% (0.60)	100% (0.58)	87% (0.57)	1% (-)	100% (0.51)	100% (0.54)
	Time/Freq.	100% (0.75)	58% (0.75)	36% (-)	100% (0.72)	100% (0.77)	40% (-)	0% (-)	65% (0.87)	98% (0.57)
	Difference	90% (0.67)	90% (0.56)	94% (0.09)	90% (0.68)	90% (0.68)	90% (0.64)	86% (0.94)	92% (0.51)	95% (0.14)
	Min Zero	79% (0.90)	62% (0.80)	80% (0.81)	70% (0.90)	77% (0.90)	41% (-)	2% (-)	74% (0.70)	66% (0.70)

Table 2: ResNet: The first number is the faithfulness and the number in the parenthesis is the sparsity metric.

frequency domain in 6 out of 8 faithful methods, as it was shown in Figure 1a and 1b. As we speculated, both ECG-FiveDays and ECG5000 are sparsest in difference space for most XAI methods.⁶ The last three datasets, LargeKitchenAppliance, ElectricDevices, and Earthquakes, are examples of datasets where the original zero value (before normalization) correspond to the lack of feature and, hence, min zero space is the most sparse space across most XAI methods. Overall, the only exception we encounter was the GunPoint dataset where we initially hypothesized that the difference space is the most appropriate due to the nature of the dataset, containing hand movement. However, by comparing time and frequency domains (as depicted in Figure 2e and 2f), it is evident that only the first few frequency com-

⁶Note that we exclude experiment with time/frequency domain in datasets where the number of time steps is small because it was impossible to get a better resolution than the frequency domain.

ponents are non-negligible and others are relatively small. Hence, we speculate that for datasets containing only low frequencies, any XAI method is likely to be more sparse in the frequency space. Due to the lack of space, the results for InceptionTime is provided in Appendix. Overall, we observe the same pattern.

Robustness on Different Spaces

The results of robustness for ResNet model is shown in Table 3. Due to the lack of space, we only show one dataset for each dataset type. See Appendix for results on other datasets and also InceptionTime model. Unlike sparsity metric, there is no strong correlation between dataset types and robustness. However, there are a few observations worth considering: First, classifier robustness does not necessarily match the XAI robustness. For example, the time domain is the most robust space in ECG5000 while the XAI robustness

Dataset	Domain	Classifier	XAI Robustness ($\times 10^{-4}$)								
			Robustness	DeepLIFT	GradientSHAP	G. Backprop	I \times G	IG	Kernel SHAP	LIME	Occlusion
AudioMNIST	Time	73.7	3.7	13.5	4.9	5.5	3.4	14.4	6.3	4.0	24.3
	Freq.	85.5	7.0	9.4	2.0	8.3	3.0	10.6	6.8	10.0	11.6
	Time/Freq.	18.9	0.6	5.7	0.3	1.1	0.5	11.3	3.1	0.7	5.5
	Difference	46.8	4.4	13.9	16.0	4.6	5.3	14.4	6.9	3.3	37.4
	Min Zero	78.3	18.3	23.0	5.0	24.5	16.1	23.8	6.7	0.8	24.6
FordA	Time	2.5	12.6	81.6	13.5	19.3	13.2	108.8	51.7	3.6	27.0
	Freq.	2.6	1.1	34.8	0.8	1.9	1.0	79.1	39.5	2.2	2.6
	Time/Freq.	4.2	1.7	24.7	1.8	3.0	1.1	57.6	23.5	1.0	3.8
	Difference	19.7	20.2	92.3	38.3	44.2	22.6	66.7	56.2	4.0	96.6
	Min Zero	2.6	17.9	81.9	13.7	27.0	20.8	115.0	53.2	0.2	27.2
GunPoint	Time	15.2	129.5	174.9	43.7	157.8	160.2	201.9	177.2	17.9	152.7
	Freq.	7.0	6.8	61.3	2.0	23.1	13.6	196.5	163.2	5.9	26.8
	Difference	3.6	5.6	175.5	12.2	19.3	6.8	217.6	178.1	9.5	43.3
	Min Zero	16.0	55.7	171.2	43.1	93.6	77.3	207.1	175.2	12.3	152.2
ECG5000	Time	4.2	35.5	160.5	44.8	72.1	35.7	237.5	188.4	22.6	94.0
	Freq.	4.7	8.2	99.5	5.3	24.2	10.1	201.0	186.5	20.2	34.5
	Difference	6.0	2.7	63.4	31.0	9.2	10.0	214.3	185.6	4.8	60.3
	Min Zero	5.0	69.8	188.6	51.4	100.8	76.9	241.4	191.1	4.9	102.8
LargeKit-App.	Time	5.1	1.7	30.1	2.5	2.9	1.5	87.3	36.2	3.3	13.8
	Freq.	22.4	14.7	31.3	7.5	19.7	5.7	56.8	37.3	3.2	24.5
	Time/Freq.	3.0	1.2	16.0	0.9	2.2	1.2	45.6	13.1	0.6	2.3
	Difference	157.7	6.4	26.1	66.9	5.0	6.1	92.1	39.9	1.2	81.6
	Min Zero	5.0	1.4	30.3	2.5	2.8	1.5	54.4	35.8	2.6	13.8

Table 3: Robustness (ResNet)

on time domain are among the worst. Interestingly, whenever time/frequency is provided for a dataset, XAI methods on this space are among the most robust ones (20 out of 27). Unlike the classifier robustness where the min zero space and time domain perform similarly, their XAI robustness can be vastly different due to the way they handle the baseline. Overall, no clear indication can be given on the best explanation space purely based on the robustness.

Discussion

Unlike computer vision, time series data is an umbrella term covering vastly different applications with widely different characteristics. This includes stock market data, EEG signal, audio signals, accelerometer data, as well as non-temporal data, such as spectrogram (e.g. Beef and Coffee dataset in UCR repository) or skeleton(contour)-based descriptors (e.g. ArrowHead or Fish datasets). Application-specific experts often rely on domain-specific knowledge for time series analysis that is absent and disconnected from the computer science community. This leads to the proliferation of classification and explanation methods that do not take application specific nuances into account (e.g. the usage of different spaces/domains.). While the application-blind approach has often worked largely for classifications due to the power DL, it faces significant challenges when it comes to explanation.

In this paper, we bridge the gap between application-blind approaches in computer science community and the application-specific approaches used by domain experts.

Our method allows computer scientists to continue proposing application-blind XAI methods without worrying about the explanation space. Interdisciplinary researchers can now focus on proposing new mappings to project known spaces to desired, yet ignored, spaces, to facilitate the usage of existing XAI. Finally, our framework allows domain experts to easily explore other spaces and investigate if there exists a better space for explanation, similar to what we have observed from GunPoint dataset where frequency domain tends to provide more sparser explanation rather than the hypothesized difference space. This can also help practitioners to investigate what features a model uses. As shown in (Vielhaben et al. 2024), a model that exploits average value of the entire time series is hard to catch in time domain. However, it can be easily identified by checking the first frequency component of the frequency space.

Conclusion

In this paper, we introduce a wrapping process that allows a model trained on one domain to operate on other domains and, thus, allows existing XAI methods to explain the model in different input domains. We suggest four new spaces. Moreover, we introduce a new sparsity metric satisfying a few desirable properties. Using the proposed metric, we show that different explanation spaces can be useful for different types of time series consistent with domain knowledge and intuition. This simple yet effective technique allows a practitioner familiar with a time series in hand to easily pick the appropriate explanation space and explain the

trained classifier using any existing XAI methods.

References

- Bach, S.; Binder, A.; Montavon, G.; Klauschen, F.; Müller, K.-R.; and Samek, W. 2015. On pixel-wise explanations for non-linear classifier decisions by layer-wise relevance propagation. *PloS one*, 10(7): e0130140.
- Becker, S.; Vielhaben, J.; Ackermann, M.; Müller, K.-R.; Lapuschkin, S.; and Samek, W. 2023. AudioMNIST: Exploring Explainable Artificial Intelligence for audio analysis on a simple benchmark. *Journal of the Franklin Institute*.
- Dau, H. A.; Bagnall, A.; Kamgar, K.; Yeh, C.-C. M.; Zhu, Y.; Gharghabi, S.; Ratanamahatana, C. A.; and Keogh, E. 2019. The UCR time series archive. *IEEE/CAA Journal of Automatica Sinica*, 6(6): 1293–1305.
- Doddaiah, R.; Parvatharaju, P.; Rundensteiner, E.; and Hartvigsen, T. 2022. Class-specific explainability for deep time series classifiers. In *2022 IEEE International conference on data mining (ICDM)*, 101–110. IEEE.
- Early, J.; Cheung, G. K.; Cutajar, K.; Xie, H.; Kandola, J.; and Twomey, N. 2023. Inherently interpretable time series classification via multiple instance learning. *arXiv preprint arXiv:2311.10049*.
- Erion, G.; Joseph, D. J.; Sturmfels, P.; Lundberg, S. M.; and Lee, S.-I. 2020. Learning explainable models using attribution priors.(2019). *CoRR, abs/1906.10670*.
- Guillemé, M.; Masson, V.; Rozé, L.; and Termier, A. 2019. Agnostic local explanation for time series classification. In *2019 IEEE 31st international conference on tools with artificial intelligence (ICTAI)*, 432–439. IEEE.
- Höllig, J.; Kulbach, C.; and Thoma, S. 2022. Tsevo: Evolutionary counterfactual explanations for time series classification. In *2022 21st IEEE International Conference on Machine Learning and Applications (ICMLA)*, 29–36. IEEE.
- Höllig, J.; Thoma, S.; and Grimm, F. 2023. XTSC-bench: quantitative benchmarking for explainers on time series classification. In *2023 International Conference on Machine Learning and Applications (ICMLA)*, 1126–1131. IEEE.
- Hyndman, R. J.; and Athanasopoulos, G. 2018. *Forecasting: principles and practice*. OTexts.
- Ismail, A. A.; Gunady, M.; Corrada Bravo, H.; and Feizi, S. 2020. Benchmarking deep learning interpretability in time series predictions. *Advances in neural information processing systems*, 33: 6441–6452.
- Ismail Fawaz, H.; Lucas, B.; Forestier, G.; Pelletier, C.; Schmidt, D. F.; Weber, J.; Webb, G. I.; Idoumghar, L.; Muller, P.-A.; and Petitjean, F. 2020. Inceptiontime: Finding alexnet for time series classification. *Data Mining and Knowledge Discovery*, 34(6): 1936–1962.
- Kokhlikyan, N.; Miglani, V.; Martin, M.; Wang, E.; Alsallakh, B.; Reynolds, J.; Melnikov, A.; Kliushkina, N.; Araya, C.; Yan, S.; et al. 2020. Captum: A unified and generic model interpretability library for pytorch. *arXiv preprint arXiv:2009.07896*.
- Löffler, C.; Lai, W.-C.; Eskofier, B.; Zanca, D.; Schmidt, L.; and Mutschler, C. 2022. Don’t Get Me Wrong: How to Apply Deep Visual Interpretations to Time Series. *arXiv preprint arXiv:2203.07861*.
- Lundberg, S. M.; and Lee, S.-I. 2017. A unified approach to interpreting model predictions. *Advances in neural information processing systems*, 30.
- Parvatharaju, P. S.; Doddaiah, R.; Hartvigsen, T.; and Rundensteiner, E. A. 2021. Learning saliency maps to explain deep time series classifiers. In *Proceedings of the 30th ACM international conference on information & knowledge management*, 1406–1415.
- Queen, O.; Hartvigsen, T.; Koker, T.; He, H.; Tsiligkaridis, T.; and Zitnik, M. 2024. Encoding time-series explanations through self-supervised model behavior consistency. *Advances in Neural Information Processing Systems*, 36.
- Rezaei, S.; and Liu, X. 2020. Multitask learning for network traffic classification. In *2020 29th International Conference on Computer Communications and Networks (ICCCN)*, 1–9. IEEE.
- Ribeiro, M. T.; Singh, S.; and Guestrin, C. 2016. ” Why should i trust you?” Explaining the predictions of any classifier. In *Proceedings of the 22nd ACM SIGKDD international conference on knowledge discovery and data mining*, 1135–1144.
- Samek, W.; Montavon, G.; Vedaldi, A.; Hansen, L. K.; and Müller, K.-R. 2019. *Explainable AI: interpreting, explaining and visualizing deep learning*, volume 11700. Springer Nature.
- Schlegel, U.; Arnout, H.; El-Assady, M.; Oelke, D.; and Keim, D. A. 2019. Towards a rigorous evaluation of XAI methods on time series. In *2019 IEEE/CVF International Conference on Computer Vision Workshop (ICCVW)*, 4197–4201. IEEE.
- Schröder, M.; Zamanian, A.; and Ahmidi, N. 2023. What about the Latent Space? The Need for Latent Feature Saliency Detection in Deep Time Series Classification. *Machine Learning and Knowledge Extraction*, 5(2): 539–559.
- Shrikumar, A.; Greenside, P.; and Kundaje, A. 2017. Learning important features through propagating activation differences. In *International conference on machine learning*, 3145–3153. PMIR.
- Shrikumar, A.; Greenside, P.; Shcherbina, A.; and Kundaje, A. 2016. Not just a black box: Learning important features through propagating activation differences. *arXiv preprint arXiv:1605.01713*.
- Simonyan, K.; Vedaldi, A.; and Zisserman, A. 2013. Deep inside convolutional networks: Visualising image classification models and saliency maps. *arXiv preprint arXiv:1312.6034*.
- Springenberg, J. T.; Dosovitskiy, A.; Brox, T.; and Riedmiller, M. 2014. Striving for simplicity: The all convolutional net. *arXiv preprint arXiv:1412.6806*.
- Sundararajan, M.; Taly, A.; and Yan, Q. 2017. Axiomatic attribution for deep networks. In *International conference on machine learning*, 3319–3328. PMLR.

Suresh, H.; Hunt, N.; Johnson, A.; Celi, L. A.; Szolovits, P.; and Ghassemi, M. 2017. Clinical intervention prediction and understanding using deep networks. *arXiv preprint arXiv:1705.08498*.

Vielhaben, J.; Lapuschkin, S.; Montavon, G.; and Samek, W. 2024. Explainable ai for time series via virtual inspection layers. *Pattern Recognition*, 150: 110309.

Zeiler, M. D.; and Fergus, R. 2014. Visualizing and understanding convolutional networks. In *Computer Vision–ECCV 2014: 13th European Conference, Zurich, Switzerland, September 6–12, 2014, Proceedings, Part I 13*, 818–833. Springer.

Appendices

Explanation Space Implementation

The representation space function, $F(x)$, is used outside a neural network and it can be construed as a pre-processing stage (with respect to the explanation generation stage at inference time, not with respect to training stage). Hence, the target domain data, $z = F(x)$, can be obtained by implementing the transformation in any arbitrary way. However, $F^{-1}(z)$ function is embedded into the M' neural network. Hence, for compatibility with gradient-based methods, we either need to use the existing functions in deep learning packages or implement the function using existing layers. Fortunately, most packages, like PyTorch, has the implementation of FFT, STFT (through torchaudio.transforms.Spectrogram), and their inverse. We implement inverse mapping function for min zero space and difference space using a single fully connected layer with a pre-defined weight matrix, as follows:

Min Zero Space Implementation: The inverse mapping of the min zero space can be written as follows:

$$F_{min_zero}^{-1}(\{x_1 - x_{min}, \dots, x_N - x_{min}, x_{min}\}) \rightarrow \{x_1, x_2, \dots, x_N\} \quad (7)$$

In terms of a fully connected layer, it can be implemented as a layer that takes a vector of size $N + 1$ as input and output a vector of size N , where the $(N + 1)^{th}$ element is added to all other elements in the input vector and then it is dropped from the output. It can be easily shown that an Identity matrix of size $N \times N$ concatenated to an all-one matrix of size $1 \times N$ can obtain the reverse mapping as a linear layer as follows:

$$\begin{aligned} \begin{bmatrix} x_1 - x_{min} \\ x_2 - x_{min} \\ \dots \\ x_{N-1} - x_{min} \\ x_N - x_{min} \\ x_{min} \end{bmatrix}_{N+1 \times 1}^T & \begin{bmatrix} 1 & 0 & \dots & 0 & 0 \\ 0 & 1 & \dots & 0 & 0 \\ \dots & \dots & \dots & \dots & \dots \\ 0 & 0 & \dots & 1 & 0 \\ 0 & 0 & \dots & 0 & 1 \\ 1 & 1 & \dots & 1 & 1 \end{bmatrix}_{N+1 \times N} \\ & = \begin{bmatrix} x_1 \\ x_2 \\ \dots \\ x_{N-1} \\ x_N \end{bmatrix}_{N \times 1}^T \end{aligned} \quad (8)$$

Difference Space Implementation: The inverse mapping of the difference space can be written as follows:

$$F_{diff}^{-1}(\{x_1, x_2 - x_1, x_3 - x_2, \dots, x_N - x_{N-1}\}) \rightarrow \{x_1, x_2, \dots, x_N\} \quad (9)$$

It can be easily shown that the i^{th} elements of the output can be obtained by adding all previous input elements up to i^{th} element. As a result, all 1 to $i - 1$ elements are cancel out and only the x_i remains which constructs the inverse operation. In linear layer with matrix multiplication operation, it can be easily implemented by a weight matrix of upper triangular form where every non-zero element is exactly one, as follow:

$$\begin{aligned} \begin{bmatrix} x_1 \\ x_2 - x_1 \\ \dots \\ x_{N-1} - x_{N-2} \\ x_N - x_{N-1} \end{bmatrix}_{N \times 1}^T & \begin{bmatrix} 1 & 1 & \dots & 1 & 1 \\ 0 & 1 & \dots & 1 & 1 \\ \dots & \dots & \dots & \dots & \dots \\ 0 & 0 & \dots & 1 & 1 \\ 0 & 0 & \dots & 0 & 1 \end{bmatrix}_{N \times N} \\ & = \begin{bmatrix} x_1 \\ x_2 \\ \dots \\ x_{N-1} \\ x_N \end{bmatrix}_{N \times 1}^T \end{aligned} \quad (10)$$

What Is β In Sparsity?

In the sparsity metric, $\beta > 1$ is a constant hyper-parameter to spread out the metric more uniformly. Empirically, for majority of datasets/XAIs, the attribution is relatively sparse and it is rarely uniformly distributed. Consequently, in most cases, all methods give a value between 0.90 and 1 which makes it hard to compare one another. Hence, choosing $\beta > 1$ allows us to better spread out the values and compare XAI Methods.

Sparsity/Faithfulness Results on InceptionTime

The results of the InceptionTime model is presented in Table 4. The results are similar to ResNet model. For example, AudioMNIST is mostly sparse on time/frequency and frequency domains. FordA is mostly sparse on frequency domain and so on.

Robustness Results

The rest of the robustness results on ResNet is shown in Table 5. The results of classifier robustness and XAI robustness is presented in Table 6. The overall patterns are similar to ResNet.

Reproducibility Checklist

This paper:

- Includes a conceptual outline and/or pseudocode description of AI methods introduced (yes/partial/no/NA)? **Yes.**
- Clearly delineates statements that are opinions, hypothesis, and speculation from objective facts and results (yes/no) **Yes.**

Dataset	Domain	DeepLIFT	GradientSHAP	G. Backprop	$I \times G$	IG	Kernel SHAP	LIME	Occlusion	Saliency
AudioMNIST	Time	66% (0.91)	87% (0.85)	80% (0.78)	86% (0.88)	87% (0.88)	78% (0.79)	0% (-)	92% (0.77)	93% (0.75)
	Freq.	83% (0.93)	89% (0.91)	97% (0.91)	92% (0.89)	90% (0.88)	68% (0.89)	21% (-)	92% (0.72)	98% (0.83)
	Time/Freq.	65% (0.97)	97% (0.93)	99% (0.88)	95% (0.95)	85% (0.93)	89% (0.78)	18% (-)	100% (0.96)	90% (0.83)
	Difference	91% (0.86)	100% (0.82)	80% (0.12)	100% (0.86)	100% (0.87)	100% (0.91)	62% (0.99)	100% (0.72)	100% (0.07)
	Min Zero	88% (0.71)	100% (0.67)	97% (0.78)	99% (0.75)	100% (0.70)	97% (0.70)	34% (-)	89% (0.91)	96% (0.75)
FordA	Time	0% (-)	42% (-)	42% (0.29)	43% (-)	42% (-)	43% (-)	7% (-)	47% (-)	44% (-)
	Freq.	0% (-)	62% (0.88)	79% (0.92)	83% (0.91)	90% (0.89)	47% (-)	16% (-)	74% (0.88)	51% (0.88)
	Time/Freq.	0% (-)	60% (0.86)	62% (0.80)	99% (0.89)	84% (0.85)	66% (0.63)	15% (nan)	78% (0.92)	92% (0.78)
	Difference	0% (-)	42% (-)	23% (-)	42% (-)	42% (-)	43% (-)	42% (-)	43% (0.37)	43% (-)
	Min Zero	0% (-)	42% (-)	42% (-)	42% (-)	42% (-)	42% (-)	34% (-)	42% (-)	42% (-)
GunPoint	Time	42% (-)	48% (-)	70% (0.47)	48% (-)	48% (-)	48% (-)	48% (-)	72% (0.22)	48% (-)
	Freq.	30% (-)	52% (0.86)	96% (0.91)	50% (0.90)	96% (0.90)	72% (0.47)	50% (0.85)	94% (0.84)	94% (0.86)
	Difference	72% (0.59)	70% (0.52)	48% (0.24)	70% (0.57)	70% (0.67)	68% (0.49)	60% (0.82)	70% (0.51)	70% (0.08)
	Min Zero	48% (-)	48% (-)	48% (-)	48% (-)	48% (-)	48% (-)	44% (-)	48% (-)	48% (-)
ECGFiveDays	Time	65% (0.83)	87% (0.73)	100% (0.66)	96% (0.79)	100% (0.78)	57% (0.42)	39% (-)	100% (0.70)	52% (0.44)
	Freq.	65% (0.70)	83% (0.73)	96% (0.70)	100% (0.72)	100% (0.74)	87% (0.38)	26% (-)	91% (0.72)	100% (0.70)
	Difference	61% (0.83)	65% (0.78)	70% (0.18)	70% (0.80)	35% (-)	91% (0.48)	96% (0.81)	100% (0.74)	83% (0.21)
	Min Zero	61% (0.67)	83% (0.65)	100% (0.66)	100% (0.55)	100% (0.56)	61% (0.40)	52% (0.80)	100% (0.26)	87% (0.44)
ECG5000	Time	68% (0.66)	81% (0.59)	96% (0.52)	95% (0.61)	89% (0.69)	75% (0.52)	9% (-)	99% (0.59)	100% (0.38)
	Freq.	43% (-)	69% (0.74)	99% (0.83)	93% (0.80)	95% (0.71)	75% (0.49)	24% (-)	89% (0.72)	100% (0.74)
	Difference	100% (0.81)	99% (0.63)	100% (0.03)	100% (0.76)	100% (0.77)	93% (0.53)	40% (-)	100% (0.54)	100% (0.07)
	Min Zero	100% (0.53)	100% (0.51)	100% (0.53)	100% (0.43)	100% (0.51)	100% (0.42)	93% (0.81)	100% (0.15)	100% (0.38)
LargeKit.App.	Time	43% (-)	66% (0.93)	66% (0.80)	70% (0.94)	65% (0.95)	73% (0.69)	11% (-)	94% (0.86)	87% (0.70)
	Freq.	53% (0.81)	75% (0.81)	92% (0.70)	87% (0.85)	85% (0.81)	56% (0.68)	2% (-)	95% (0.69)	97% (0.82)
	Time/Freq.	74% (0.97)	68% (0.92)	43% (-)	95% (0.94)	97% (0.96)	52% (0.67)	23% (-)	64% (0.83)	76% (0.78)
	Difference	87% (0.97)	84% (0.92)	47% (-)	84% (0.96)	84% (0.96)	91% (0.57)	26% (-)	97% (0.91)	95% (0.09)
	Min Zero	45% (-)	63% (0.93)	66% (0.80)	67% (0.96)	61% (0.96)	57% (0.69)	13% (-)	84% (0.91)	64% (0.70)
ElectricDev.	Time	83% (0.67)	90% (0.61)	83% (0.25)	90% (0.67)	95% (0.64)	89% (0.36)	59% (0.77)	72% (0.26)	100% (0.42)
	Freq.	95% (0.74)	91% (0.52)	99% (0.51)	85% (0.51)	97% (0.53)	92% (0.45)	78% (0.76)	97% (0.28)	99% (0.45)
	Difference	99% (0.64)	68% (0.63)	46% (-)	92% (0.66)	88% (0.65)	98% (0.45)	79% (0.73)	93% (0.49)	96% (0.11)
	Min Zero	81% (0.80)	81% (0.67)	83% (0.25)	79% (0.79)	89% (0.75)	70% (0.43)	51% (0.75)	82% (0.65)	88% (0.42)
Earthquakes	Time	16% (-)	53% (0.69)	64% (0.48)	56% (0.72)	58% (0.76)	17% (-)	4% (-)	45% (-)	44% (-)
	Freq.	17% (-)	47% (-)	18% (-)	93% (0.65)	95% (0.64)	17% (-)	3% (-)	82% (0.53)	40% (-)
	Time/Freq.	79% (0.75)	46% (-)	22% (-)	86% (0.73)	83% (0.72)	28% (-)	5% (-)	52% (0.47)	86% (0.49)
	Difference	15% (-)	15% (-)	16% (-)	15% (-)	15% (-)	15% (-)	15% (-)	16% (-)	30% (-)
	Min Zero	16% (-)	42% (-)	90% (0.48)	51% (0.83)	51% (0.84)	18% (-)	5% (0.95)	41% (-)	44% (-)

Table 4: InceptionTime: The first number is the faithfulness success percentage (SP), *Faith*, and the number in the parenthesis is the sparsity metric.

- Provides well marked pedagogical references for less-familiare readers to gain background necessary to replicate the paper (yes/no) **Yes**.

Does this paper make theoretical contributions? (yes/no) **No**.

Does this paper rely on one or more datasets? (yes/no) **Yes**.

If yes, please complete the list below.

- A motivation is given for why the experiments are conducted on the selected datasets (yes/partial/no/NA) **Yes**.
- All novel datasets introduced in this paper are included in a data appendix. (yes/partial/no/NA) **No. They are publicly available**
- All novel datasets introduced in this paper will be made publicly available upon publication of the paper with a li-

cense that allows free usage for research purposes. (yes/partial/no/NA) **NA**.

- All datasets drawn from the existing literature (potentially including authors' own previously published work) are accompanied by appropriate citations. (yes/no/NA) **Yes**.
- All datasets drawn from the existing literature (potentially including authors' own previously published work) are publicly available. (yes/partial/no/NA) **Yes**.
- All datasets that are not publicly available are described in detail, with explanation why publicly available alternatives are not scientifically satisfying. (yes/partial/no/NA) **NA**.

Does this paper include computational experiments? (yes/no) **Yes**.

If yes, please complete the list below.

Dataset	Domain	Classifier	XAI Robustness ($\times 10^{-4}$)								
			Robustness	DeepLIFT	GradientSHAP	G. Backprop	I \times G	IG	Kernel SHAP	LIME	Occlusion
ECGFiveDays	Time	7.1	13.0	122.5	22.9	18.6	11.2	242.9	188.2	13.5	98.6
	Freq.	15.6	35.4	111.1	10.5	44.6	16.5	182.5	190.6	11.4	49.7
	Difference	19.0	36.9	92.7	37.3	43.4	24.0	218.5	199.9	13.5	188.7
	Min Zero	10.4	94.3	152.7	29.0	111.4	86.5	253.0	195.0	12.2	114.1
ElectricDev.	Time	28.9	39.7	189.7	14.1	156.0	43.5	309.6	223.7	31.0	237.2
	Freq.	217.5	127.2	190.5	32.5	160.1	69.0	253.7	220.0	96.9	173.9
	Difference	111.6	70.8	140.7	257.5	96.4	59.3	276.4	275.3	42.8	306.6
	Min Zero	29.4	12.0	163.4	14.1	38.4	13.5	284.8	236.2	12.7	236.1
Earthquakes	Time	1.3	1.4	56.2	1.7	4.1	2.2	59.7	39.5	2.0	6.9
	Freq.	2.6	3.7	67.6	2.9	8.0	4.2	76.5	34.8	5.7	10.7
	Time/Freq.	0.3	1.9	34.1	1.3	4.3	1.7	53.5	35.9	1.0	4.5
	Difference	35.0	27.3	83.2	35.1	41.1	38.2	80.4	55.2	8.0	97.2
	Min Zero	1.3	1.3	57.9	1.7	3.8	2.1	65.1	43.1	1.8	6.9

Table 5: Robustness (ResNet)

- Any code required for pre-processing data is included in the appendix. (yes/partial/no) **Yes**.
- All source code required for conducting and analyzing the experiments is included in a code appendix. (yes/partial/no) **Yes**.
- All source code required for conducting and analyzing the experiments will be made publicly available upon publication of the paper with a license that allows free usage for research purposes. (yes/partial/no) **Yes**.
- All source code implementing new methods have comments detailing the implementation, with references to the paper where each step comes from (yes/partial/no) **Partial**.
- If an algorithm depends on randomness, then the method used for setting seeds is described in a way sufficient to allow replication of results. (yes/partial/no/NA) **Yes**. **All experiments are started by setting the randomness seed to zero**.
- This paper specifies the computing infrastructure used for running experiments (hardware and software), including GPU/CPU models; amount of memory; operating system; names and versions of relevant software libraries and frameworks. (yes/partial/no) **No**.
- This paper formally describes evaluation metrics used and explains the motivation for choosing these metrics. (yes/partial/no) **Yes**.
- This paper states the number of algorithm runs used to compute each reported result. (yes/no) **Yes**.
- Analysis of experiments goes beyond single-dimensional summaries of performance (e.g., average; median) to include measures of variation, confidence, or other distributional information. (yes/no) **No**.
- The significance of any improvement or decrease in performance is judged using appropriate statistical tests (e.g., Wilcoxon signed-rank). (yes/partial/no) **No**.
- This paper lists all final (hyper-)parameters used for each model/algorithm in the paper’s experiments. (yes/partial/no/NA) **Partial**.
- This paper states the number and range of values tried per (hyper-) parameter during development of the paper, along with the criterion used for selecting the final parameter setting. (yes/partial/no/NA) **Partial**.

Dataset	Domain	Classifier	XAI Robustness ($\times 10^{-4}$)								
			Robustness	DeepLIFT	GradientSHAP	G. Backprop	I \times G	IG	Kernel SHAP	LIME	Occlusion
AudioMNIST	Time	37.9	2.0	11.4	2.7	3.6	2.6	14.4	6.3	1.5	23.7
	Freq.	12.9	4.1	8.5	0.9	5.8	1.9	13.1	6.8	4.1	8.2
	Time/Freq.	17.9	0.5	4.9	0.3	0.5	0.3	12.6	3.1	0.3	3.3
	Difference	99.3	1.7	9.3	40.9	2.6	1.4	11.8	7.0	6.1	32.6
	Min Zero	40.4	23.5	23.8	2.8	23.4	17.7	23.5	6.5	0.4	23.9
FordA	Time	1.7	nan	81.7	14.7	15.5	13.2	93.6	52.2	3.3	20.6
	Freq.	2.2	nan	37.3	0.9	2.5	1.0	78.2	46.2	2.2	3.5
	Time/Freq.	7.5	nan	23.3	3.9	2.9	1.2	55.8	22.8	0.9	3.2
	Difference	13.2	nan	82.9	82.9	45.9	26.1	78.9	57.0	4.1	97.2
	Min Zero	1.9	nan	81.4	14.9	18.3	16.5	118.0	53.7	0.2	20.8
GunPoint	Time	6.9	53.7	149.3	54.9	133.9	117.3	245.5	180.0	12.4	124.9
	Freq.	9.9	3.0	63.3	1.1	5.6	4.2	194.6	113.1	5.7	6.2
	Difference	5.8	5.5	146.8	5.8	5.7	7.5	207.8	177.5	5.6	13.6
	Min Zero	7.1	70.8	154.3	54.5	89.8	78.4	245.2	177.1	7.6	124.1
ECGFiveDays	Time	0.1	6.1	108.7	7.4	6.8	6.1	208.6	168.7	0.9	26.5
	Freq.	0.3	16.8	102.1	3.7	7.9	3.8	207.9	173.8	4.4	10.1
	Difference	0.6	5.3	94.1	49.2	24.1	26.0	226.7	172.2	3.4	88.3
	Min Zero	0.2	33.4	117.7	9.8	25.9	20.4	238.2	197.9	1.8	34.2
ECG5000	Time	0.8	29.4	134.8	20.4	29.4	17.6	169.5	188.6	4.1	60.3
	Freq.	1.8	17.2	92.0	2.8	9.0	3.9	189.9	172.6	7.0	13.5
	Difference	3.6	2.2	84.2	5.6	5.2	2.0	213.3	182.7	8.3	22.1
	Min Zero	1.0	62.7	162.0	23.3	60.3	37.0	218.6	190.0	3.8	66.9
LargeKit.App.	Time	2.7	10.0	20.7	5.8	5.6	5.0	54.2	37.2	0.7	20.4
	Freq.	5.4	8.1	25.6	6.4	13.2	5.3	58.1	37.2	4.5	14.1
	Time/Freq.	1.7	1.6	15.2	3.8	1.2	0.6	44.0	14.7	0.6	1.5
	Difference	60.8	6.9	26.1	80.9	4.9	4.9	84.3	38.9	3.0	78.0
	Min Zero	2.6	10.1	20.8	5.8	5.5	4.8	55.2	37.1	0.5	20.4
ElectricDev.	Time	292.5	45.1	213.4	137.3	127.8	101.5	291.3	217.2	73.0	230.1
	Freq.	375.0	56.3	187.1	91.8	153.7	72.0	245.9	203.2	105.8	174.7
	Difference	291.2	56.6	123.1	51.4	114.0	58.0	282.3	265.5	72.0	310.8
	Min Zero	289.8	39.0	173.3	136.0	35.6	22.9	284.2	246.1	23.2	228.4
Earthquakes	Time	1.0	6.8	63.5	13.4	6.4	4.5	48.9	51.6	1.8	22.9
	Freq.	1.7	14.8	67.9	9.6	9.7	3.8	54.7	51.4	7.8	13.3
	Time/Freq.	1.3	7.7	38.0	4.0	4.8	2.0	47.9	20.1	1.3	5.3
	Difference	39.6	21.9	70.0	33.2	48.5	31.5	82.0	56.5	8.9	115.0
	Min Zero	0.9	6.9	65.4	13.3	4.1	2.5	47.4	51.7	1.5	22.9

Table 6: Robustness (InceptionTime)